DIURNAL VARIATIONS OF CONVECTIVE STORM IN WARM-SEASON OVER CONTIGUOUS NORTH CHINA BASED ON RADAR MOSAIC CLIMATOLOGY

Mingxuan Chen[1], Yingchun Wang [2], Feng Gao[1], Xian Xiao[1]
[1] Institute of Urban Meteorology, China Meteorological Administration, Beijing, China
[2] Beijing Meteorological Service, China Meteorological Administration, Beijing, China

ABSTRACT

1. INTRODUCTION

Both weather forecast and climate prediction are heavily dependent on adequate representation of convective precipitation and storm processes, including diurnal cycle of convection life. However, the diurnal cycle is poorly represented in today's weather and climate models. Analysis on diurnal variations of warm-season precipitation and storm is very important at least in the following three parts: 1) to understand the mechanism of both warm-season rain formation and local climatology [e.g., *Carbone et al.*, 2002; *Parker and Knievel*, 2005; *Carbone and Tuttle*, 2008; *Lin et al.*, 2011], 2) to evaluate and improve parameterization scheme and other physics, and serve as a benchmark for new representations in numerical models [e.g., *Davis et al.*, 2003; *Liang et al.*, 2004], and 3) to improve the accuracy of forecasting the timing and location of convective precipitation and storm [e.g., *Saxen et al.*, 2008].

Over the past several decades, numerous climatological studies have been performed for diurnal variations of global and regional warm-season precipitation and storm through observations from surface, radar, satellite and lightning [e.g., *Wallace*, 1975; *Reap and MacGorman*, 1989; *Steiner et al.*, 1995; *Livingston et al.*, 1996; *Carbone et al.*, 2002; *Wang et al.*, 2004; *Hsu et al.* 2006; *Carbone and Tuttle*, 2008; *Surcel et al.*, 2010]. Most of these studies have presented diurnal variations of convective precipitation or storm are high dissimilar in different parts of the world. Climatological studies on diurnal variations of warm-season precipitation over China had also been implemented to focus on the rainfall occurs over the east, center or south large-scale regions of China [e.g., *Yu et al.*, 2007a, 2007b]. However, these studies didn't emphasize the contiguous North China (i.e., Beijing and its vicinal regions) where is an important warm-season rainfall region over complex topography in China [*He and Zhang*, 2010] and also didn't use high-resolution radar data owing to absence of successive radar observations for several years. At present, radar observations have been collected since 2008 that have high spatial and temporal resolutions and good coverage from China's CINRADs in the region. In this study, radar climatology was performed to investigate diurnal variations of convective storm over the region.

2. DATA AND ANALYSIS METHODOLOGY

Following these studies given by *Carbone et al.* [2002], *Carbone and Tuttle* [2008] and *Lin et al.* [2011], radar climatology can be implemented to achieve significant variation characteristics of convective storm and precipitation in warm-season using 4-year or more weather radar data. In this paper, composite reflectivity mosaic (CRM) data will be analyzed. The data were produced using

reflectivity from operational CINRAD radars of four S-band (BJRS in Beijing, TJRS in Tianjin, SJZRS in Shijiazhuang and QHDRS in Qinhuangdao) and two C-band (ZBRC in Zhangbei and CDRC in Chengde) over the contiguous North China during 2008 – 2011 (see Figure 1 for radar sites). All of these radars were controlled for synchronization scanning under Volume Coverage Pattern 21 (VCP21) mode with approximate 6-minute interval using a radar command system at Beijing Meteorological Service. The reflectivity data on each radar polar coordinates were interpolated to produce three-dimensional (3D) reflectivity which combined to form 3D reflectivity mosaic grids and then the two-dimensional CRM data with 1-km Cartesian resolution in a square analysis domain of 600 km by 600 km that centered on the BJRS radar site (Figure 1) [*Chen et al.*, 2010].

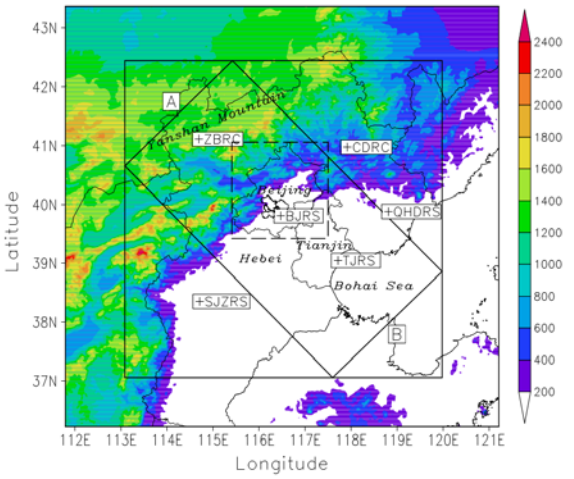

Figure 1. Topography height over the contiguous North China shaded by colors with 200-meter interval. Analysis domain of 600 km by 600 km for the radar climatology, subdomain for drawing Figure 4c, and subdomain for calculating mean storm percentage over Beijing area are marked by the solid square, the solid slantwise rectangle, and the small dashed square, respectively. Radar sites of the 6 operational CINRADs are labeled using plus signs.

For reducing clutter contamination, radar reflectivity observations were quality controlled to remove clutters before the CRM data were generated [*Chen et al.*, 2010]. The complex mountainous terrain around the two C-band radars (ZBRC and CDRC, Figure 1) resulted in evident beam blockage and ground clutter. Whereas, it was very difficult to completely restrain them and simultaneously insure true storm echoes were not influenced. Therefore, a few ground clutters from ZBRC radar still had to be remained in northwest of the domain for integrality of true storm echoes (cf., Figure 2). In addition, bright bands that frequently bring artificially high reflectivity near freezing layer [*Fabry and Zawadzki*, 1995] were also removed from the 3D reflectivity mosaic using an automatic identification algorithm [*Chen and Gao*, 2006].

In this study, the “warm-season” is defined as 15th May through 15th September. Most of convective storms occur over the contiguous North China during this period. The radar climatology is based on the CRM data of four warm-seasons from 2008 to 2011. Hourly average observation number of reflectivity more than or equal to different thresholds is calculated on each grid of 1 km by 1 km in the 600 km by 600 km domain under diurnal cycle mode. Accordingly, hourly average occurrence frequency of reflectivity above set threshold can be expressed using observation number above the relevant threshold or their percentage related to total number. Following other studies, the 40 dBZ can be considered as a reasonable reflectivity threshold criterion for convective activity [e.g., *Reap and MacGorman*, 1989; *Livingston et al.*, 1996; *Lin et al.*, 2011], and used to discriminate convective storm and stratiform rain [e.g., *Falconer*, 1984; *Parker and Knievel*, 2005]. Here, hourly average observation number of

reflectivity more than or equal to 40 dBZ is used. Note that the terrain elevation height lower than 200 meters is regarded as foothills or plains (Figure 1), and the time used refers to the universal time coordinated (UTC) that plus 8 hours is local solar time (LST).

3. RESULTS

The spatial distributions of hourly average observation number of reflectivity more than or equal to 40 dBZ are firstly analyzed for describing diurnal variations of storm occurrence frequency that indicate storm initiation or intensification over the contiguous North China. The results are shown in Figure 2 for only four UTC hours (02:00-03:00, 07:00-08:00, 10:00-11:00, 18:00-19:00) due to length limited of the paper. Beginning from 04:00 (12:00 LST), storm occurrence frequency increases obviously over the mountainous area in NW of the region, especially at 06:00-10:00, which results from thermal forcing of the mountainous area. The mountainous area as a heat source is an important storm genesis zone in the afternoon that similar to other studies [*Schaaf et al.*, 1988; *Carbone et al.*, 2002; *Lin et al.*, 2011]. Thereafter, the occurrence frequency decreases rapidly over the mountains after 11:00. During other periods, most of storms initiate and develop over the foothills or the SE plains, with distinct augment of storm occurrence frequency from 08:00. At 10:00-11:00, close relationship between storm enhancement and topography over the region is revealed in figure 2c. Especially, observation number of reflectivity more than or equal to 40 dBZ increases over 60 and has maximum near 100 in front of the mountains of Beijing area, which correspond to storm probability of approximate 2.5% and 3.6%, respectively. The results illuminate not only most of storms strengthen while they moving southeastward and going downhill but also storm initiation is frequent along the foothills, especially in Beijing area. According to other studies [*Wilson et al.*, 2007; *Chen et al.*, 2010; *Wilson et al.*, 2010], storm intensification and initiation over the foothills nearly correlated with the favorable situation of southeasterly air rising along the sidehills and airmass instability over the plains, which were frequent during the warm-season. At 11:00-13:00, the radar climatology indicates that storm cells move southeastward unceasingly and have high probability to evolve into storm line or squall line while they reaching the SE plains in Beijing, Tianjin and their vicinity areas. During 13:00-22:00, most of nocturnal convective storms occur only over the plains with decreasing frequency. The characteristics of nocturnal convection are similar to the results using satellite data by *Zheng et al.* [2007]. Based on the results given by *Yu et al.* [2007a] and *He and Zhang* [2010], the favorable mechanisms of nocturnal convection over the plains can be inferred as that solar heating air over the mountains in daytime which subsequently propagates southeastward to the plains, and the upward branch of a mountain–plain solenoidal circulation is further facilitated by the nocturnal low-level jet over the plains that contributes to a transport of warm and moist air to the area during nighttime. Note at 13:00-14:00, there is high occurrence frequency of isolated storm cells near Beijing urban area that may be relevant to urban heat island effect [*Miao et al.*, 2011]. The great majority of storms occur over the SE plains with much less frequency in the morning and forenoon (00:00-04:00) than nighttime (13:00-22:00). Note that the extreme high observation number in NW of the region results from ground clutter from

ZBRC radar which is not removed completely.

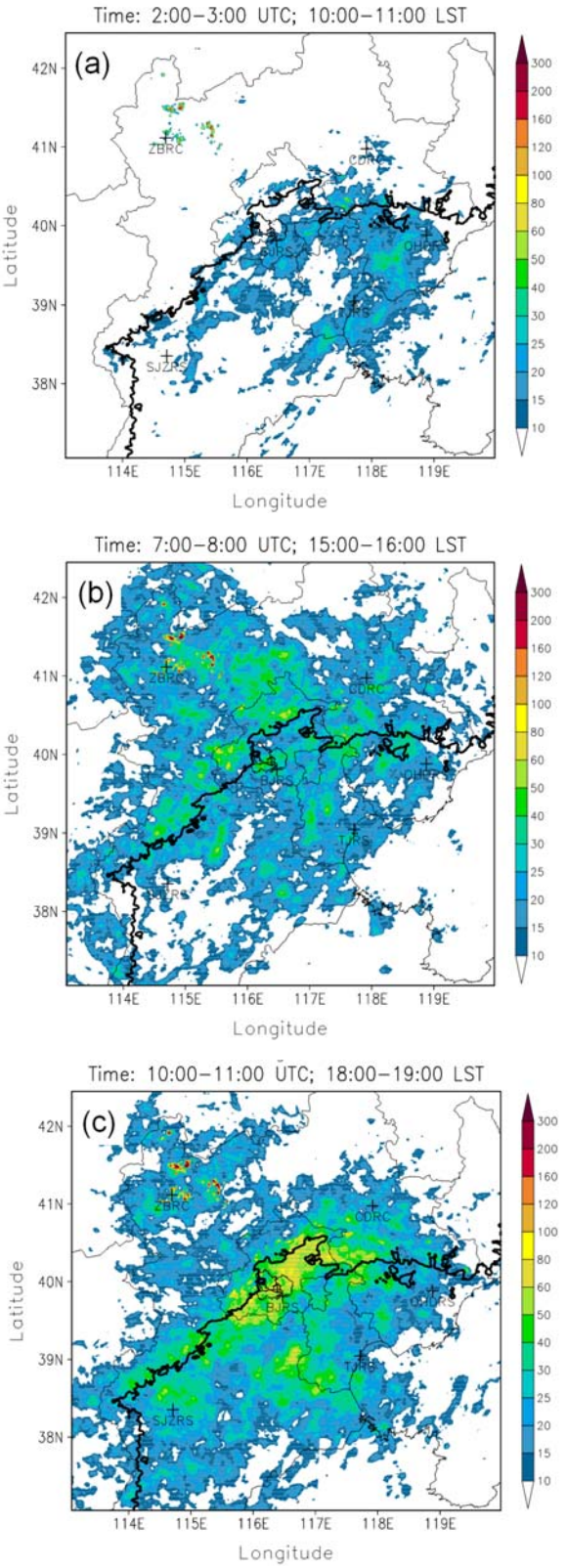

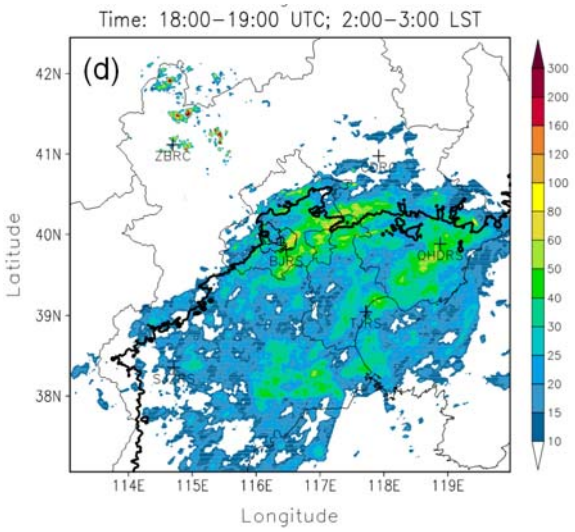

Figure 2. Spatial distributions of hourly average observation number of reflectivity more than or equal to 40 dBZ at (a) 02:00-03:00 UTC, (b) 07:00-08:00 UTC, (c) 10:00-11:00 UTC, and (d) 18:00-19:00 UTC. The thick solid line shows the 200 m terrain elevation.

To reveal the regional averaged characteristics of diurnal storm variations, Figure 3a shows diurnal mean percentage of hourly observation number of reflectivity more than or equal to 40 dBZ that averaged over the analysis domain of 600 km by 600 km. The mean percentage is much less at 02:00-05:00 than in other hour periods, but increases distinctly from 07:00. The two comparable peaks of mean percentage are denoted in the figure, with the maximal one in the late afternoon (10:00-11:00) that corresponds to the close relationship between storm enhancement activity and topography, and the other in the midnight (18:00) that corresponds to the favorable mechanism of nocturnal convection over the plains, as mentioned above. Focusing on Beijing area, Figure 3b shows mean percentage that averaged over the dashed rectangle domain marked in Figure 1. The trend of mean percentage over the contiguous Beijing area is similar to the counterpart over the contiguous North China, including much less percentage at

02:00-05:00 than at other hours, and two peaks with the maximal one at about 10:00 and the other at 18:00-20:00. The line in the Figure 3b shows the hourly number of surface stations which 24-hr rainfall exceeds 50 mm. The rain-gauge data were collected from automatic and traditional stations in Beijing area from May to September during 2008 – 2011. The diurnal trend of surface rainfall is similar to the trend of mean storm percentage and also has an analogous dual-peak, which indicates that heavy rainfall above 50 mm in 24 hours is mainly resulted from convective storm over Beijing area in the warm-season. The trend and dual-peak characteristic have discrepancy with the results using conventional surface precipitation data over contiguous China by *Yu et al.* [2007a] (see their Figure 1, 2d and 2e). The primary causation is the contiguous North China was partitioned and embraced into other two large regions (contiguous Northeast China and East China) by *Yu et al.* [2007a], which resulted in the discrepancy and similarity of diurnal precipitation variations coexist between the two large regions of *Yu et al.* [2007a] and the contiguous North China. Based on *Yu et al.* [2007b] (see their Figure 1), occurrence frequency of warm-season precipitation events of 1-3 hours was greater than 60% but rainfall amount less than 30% over the contiguous North China that were mainly contributed from short-lived convective storms. Whereas, occurrence frequency of these events last more than 6 hours was less than 15% but rainfall amount more than 50% that comprised both long-lived convective precipitation and mixed stratiform and convective precipitation. This can be regarded as another explanation for the discrepancy source. In addition, it's well-known that the climatology of storm occurrence frequency based on radar observations does not ideally correspond to which of rainfall attribute from surface observations [*Carbone and Tuttle*, 2008].

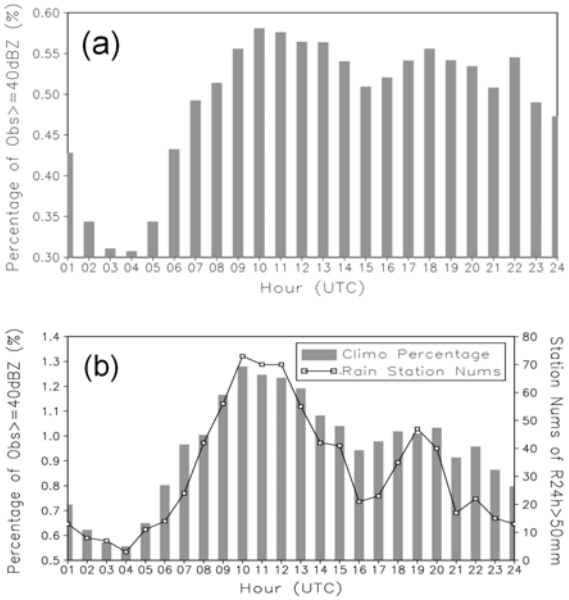

Figure 3. Mean percentage histogram of hourly observation number of reflectivity more than or equal to 40 dBZ that averaged over (a) the analysis domain for the contiguous North China and (b) the dashed rectangle domain marked in Figure 1 for Beijing area. The hourly station number of 24-hr rainfall over 50 mm is shown by the line in the (b) that collected from automatic and traditional surface stations in Beijing area from May to September during 2008 – 2011. The horizontal axis is UTC in hour.

Time-distance plot (i.e., Hovmöller diagram) of hourly average observation number of reflectivity more than or equal to 40 dBZ is used to further highlight the diurnal evolution and motion characteristics of convective storm as well as terrain effect on storm, and shown in Figure 4 that includes the averaged topographic profile. Figure 4a and 4b are respectively Hovmöller diagram of latitudinal average and longitudinal average in the domain of 600 km by 600 km, which reveal storm initiates over the mountainous area from about 04:00, and then represents propagation tendency eastward (Figure 4a) and

southward (Figure 4b). At 10:00-11:00 (late afternoon), the two Hovmöller diagrams indicate storm frequency evidently increases near the region (116ºE-117ºE, 39.5ºN-40.5ºN). It can be found that the region is just vicinity of the foothills in Beijing area where storm occurrence frequency is very high at 10:00-11:00 as mentioned above. In the next morning (about 23:00), storm dissipates rapidly near the Bohai Sea. Actually, dominating storm propagation and motion is approximately from northwest to southeast (NW-SE) over the slantwise rectangle subdomain (see Figure 1) that can be tracked using a sequential animation of hourly distributions of storm observation number. Therefore, hourly average observation number of reflectivity more than or equal to 40 dBZ were averaged in the subdomain along the A or B line that is near from southwest to northeast (SW-NE) direction to produce the Hovmöller diagram of approximate NW-SE orientation for further analysis (Figure 4c). The diagram highlights the dominating storm propagation direction is near NW-SE, and indicates the storm evolution characteristics are similar to which revealed in both latitudinal average and longitudinal average diagrams but much remarkable storm frequency that distinctly increases over the foothills at 08:00-13:00. The dominating direction of storm propagation shown in the diagram is similar to which given by *He and Zhang* [2010] (cf., their Figure 4). However, obvious discrepancies exist in other aspects due to different data, method and domain used. On average, the steeper average terrain profile corresponds to the higher increment of storm frequency by comparing the three diagrams that validates the close relationship between storm activity and topography again. The steep topography favors upslope lifting of low-level southeasterly warm-, moist-air over the foothills and plains that induces storm intensification while moving from the mountains to the plains or storm initiation along the terrain slopes and foothills [*Wilson et al.*, 2007; *Chen et al.*, 2010; *Wilson et al.*, 2010]. Note that some inconsecutive large observation number in the diagrams results from ground clutter from ZBRC radar over the mountains at 06:00-10:00 as shown in Figure 2.

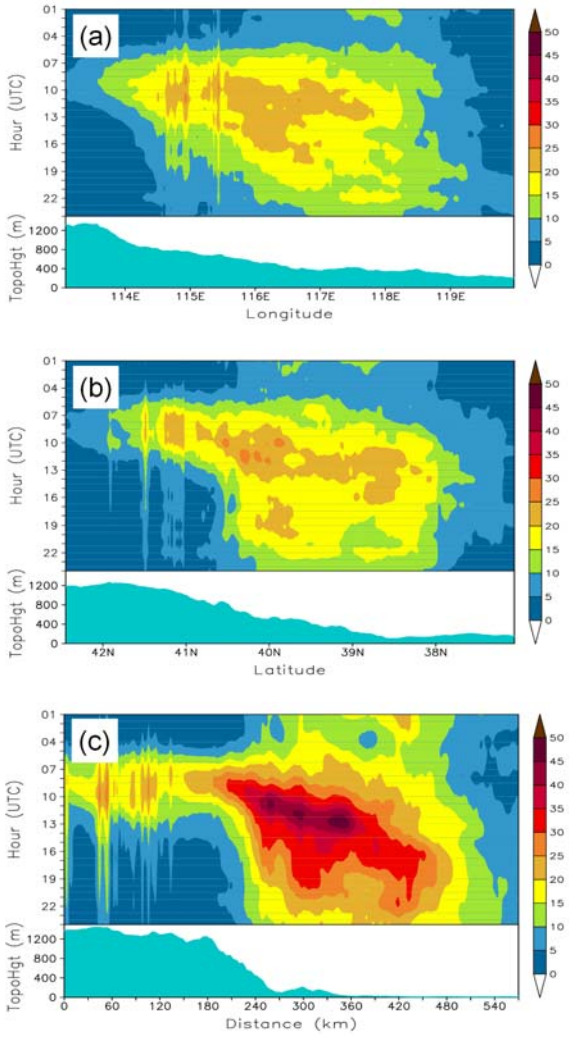

Figure 4. Hovmöller diagram of hourly average observation number of reflectivity more than or equal to 40 dBZ for (a) latitudinal average and (b) longitudinal average over the analysis domain, and (c) approximate SW-NE average along the A or B line direction over the slantwise rectangle subdomain that shown in Figure 1. The averaged topographic profile is also indicated at the bottom of each panel. The

vertical axis is UTC in hour for the Hovmöller diagrams, and elevation height in meter for the topographic profiles, respectively. The horizontal axis is approximate distance in km between A to B lines in the (c).

4. SUMMARY

Radar mosaic climatology is investigated for diurnal variations of warm-season storm over the contiguous North China using 6-min reflectivity observations from 6 CINRAD radars during 2008-2011. The results reveal the mountainous area in NW of the region is an important origin source of convective storm where has high storm frequency in the afternoon (06:00-10:00) due to solar heating but very low frequency in other hours. Most of storms propagate from the NW mountains to the SE foothills, or further to the plains. At 10:00-11:00 of the late afternoon, there is remarkable high storm occurrence frequency over the foothills, especially in the vicinity of Beijing, while storm propagates from the mountains and reach the foothills. The result indicates close relationship between storm activity and topography that the steep topography is highly advantageous to upslope lifting of low-level southeasterly warm- and moist-air over the plains which induces storm intensification and initiation along the terrain slopes and foothills. From the evening to the next early afternoon, great majority of storms only occur over the SE plains that have diminishing occurrence frequency. Hourly mean storm frequency averaged over the region indicates two comparable peaks, with maximal one in the late afternoon that related to terrain impact and the other in the nighttime that connected with favorable nocturnal convection mechanism on the plains. A similar dual-peak characteristic is found over Beijing area and validated using the statistics from surface rainfall observations.

In summertime or warm-season, there are differences of diurnal variations of convective storm and precipitation in every month or under different conditions of steering-level winds [*Carbone et al.*, 2002; Wang et al., 2004; Saxen et al., 2008]. The differences over the study region will be discussed in other papers (and may be included in the oral presentation for the symposium). In addition, direct and indirect effects of dynamical and thermal-dynamical forcing from topography, urban heat island and sea breeze on storm initiation and evolution need to be further investigated. In the near future, radar-based climatology may prove to be very powerful, important tools for forecasting convective storm and precipitation. But limitations of radar data must be better mitigated, e.g., ground clutter, beam blocking, poor calibration and range dependence [*Parker and Knievel*, 2005].

5. REFERENCES

Carbone, R. E., J. D. Tuttle, D. A. Ahijevich, and S. B. Trier (2002), Inferences of Predictability Associated with Warm Season Precipitation Episodes, J. Atmos. Sci., 59(13), 2033-2056, doi: 10.1175/1520-0469(2002)059<2033:IOPAWW>2.0.CO;2.

Carbone, R. E., and J. D. Tuttle (2008), Rainfall occurrence in the U.S. warm season: The diurnal cycle, J. Clim., 21(16), 4132-4146, doi: 10.1175/2008JCLI2275.1.

Chen, M., and F. Gao (2006), An Automatic Identification Algorithm for the Removal of Bright Band from Reflectivity of CINRAD/SA (in Chinese with English abstract), J. Appl. Meteor. Sci., 17(2), 207-214.

Chen, M., F. Gao, R. Kong, Y. Wang, J.

Wang, X. Tan, X. Xiao, W. Zhang, L. Wang, and Q. Ding (2010), Introduction of Auto Nowcasting System for Convective Storm and Its Performance in Beijing Olympics Meteorological Service (in Chinese with English abstract), J. Appl. Meteor. Sci., 21(4), 395-404.

Davis, C. A., K. W. Manning, R. E. Carbone, S. B. Trier, and J. D. Tuttle (2003), Coherence of warm-season continental precipitation in numerical weather prediction models, Mon. Weather Rev., 131(11), 2667-2679, doi: 10.1175/1520-0493(2003)131<2667:COWCRI>2.0.CO;2.

Fabry, F., and I. Zawadzki (1995), Long-term radar observations of the melting layer of precipitation and their interpretation, J. Atmos. Sci., 52(7), 838-851.

Falconer, P. D. (1984), A radar-based climatology of thunderstorm days across New York State, J. Clim. Appl. Meteor., 23(7), 1115-1120.

He, H. Z., F. Q. Zhang (2010), Diurnal Variations of Warm-Season Precipitation over Northern China, Mon. Weather Rev., 138(4), 1017-1025, doi: 10.1175/2010MWR3356.1.

Hsu H.-M., M. W. Moncrieff, W.-W. Tung, and C.H. Liu (2006), Multi-scale Temporal Variability of Warm-Season Precipitation over North America: Statistical Analysis of Radar Measurements, J. Atmos. Sci., 63(9), 2355-2368, doi: 10.1175/JAS3752.1.

Liang, X.-Z., L. Li, A. Dai, and K. E. Kunkel (2004), Regional climate model simulation of summer precipitation diurnal cycle over the United State, Geophys. Res. Lett., 31, L24208, doi:10.1029/2004GL021054.

Lin, P.-F., P.-L. Chang, B.J.-D. Jou, J.W. Wilson, and R.D. Roberts (2011), Warm Season Afternoon Thunderstorm Characteristics under Weak Synoptic-Scale Forcing over Taiwan Island, Wea. Forecasting, 26(1), 44-60, doi: 10.1175/2010WAF2222386.1.

Livingston, E. S., J. W. Nielsen-Gammon, and R. E. Orville (1996), A climatology, synoptic assessment, and thermodynamic evaluation for cloud-to-ground lightning in Georgia: A study for the 1996 Summer Olympics, Bull. Amer. Meteor. Soc., 77(7), 1483-1495.

Miao, S., F. Chen, Q. Li, and S. Fan (2011), Impacts of Urban Processes and Urbanization on Summer Precipitation: A Case Study of Heavy Rainfall in Beijing on 1 August 2006, J. Appl. Meteor. Climatol., 50(4), 806-825, doi: 10.1175/2010JAMC2513.1.

Parker, M. D., and J. C. Knievel (2005), Do meteorologists suppress thunderstorms?: Radar-derived statistics and the behavior of moist convection, Bull. Amer. Meteor. Soc., 86(3), 341-358, doi: 10.1175/BAMS-86-3-341.

Reap, R. M., and D. R. MacGorman (1989), Cloud-to-ground lightning: Climatological characteristics and relationships to model fields, radar observations, and severe local storms, Mon. Weather Rev., 117(3), 518-535.

Saxen, T. R., and Coauthors (2008), The operational mesogammascale analysis and forecast system of the U.S. Army Test and Evaluation Command. Part IV: The White Sands Missile Range Auto-Nowcast System, J. Appl. Meteor. Climatol., 47(4), 1123-1139, doi: 10.1175/2007JAMC1656.1.

Schaaf, C. B., J. Wurman, and R. M. Banta (1988), Thunderstormproducing terrain features, Bull. Amer. Meteor. Soc., 69(3), 272-277.

Steiner, M., R. A. Houze Jr., and S. E. Yuter

(1995), Climatological characterization of three-dimensional storm structure from operational radar and rain gauge data, J. Appl. Meteor., 34(9), 1978-2007.

Surcel, M., M., Berenguer, and I., Zawadzki (2010), The Diurnal Cycle of Precipitation from Continental Radar Mosaics and Numerical Weather Prediction Models. Part I: Methodology and Seasonal Comparison, Mon. Weather Rev., 138(8), 3084-3106, doi: 10.1175/2010MWR3125.1.

Wallace, J. M. (1975), Diurnal variations in precipitation and thunderstorm frequency over the conterminous United States, Mon. Weather Rev., 103(5), 406-419.

Wang, C.-C., G. T.-J. Chen, and R.E. Carbone (2004), A Climatology of Warm-season Cloud Patterns over East Asia based on GMS Infrared Brightness Temperature Observations, Mon. Weather Rev., 132(7), 1606-1629, doi: 10.1175/1520-0493(2004)132<1606:ACOWCP>2.0.CO;2.

Wilson, J. W., M. Chen, Y. Wang, and L. Wang (2007), Nowcasting Thunderstorms for the 2008 Summer Olympics, Preprints, The 33rd International Conference on Radar Meteorology, Amer. Meteor. Soc., Cairns, Australia.

Wilson, J. W., Y. Feng, M. Chen, and R.D. Roberts (2010), Nowcasting Challenges during the Beijing Olympics: Successes, Failures, and Implications for Future Nowcasting Systems, Wea. Forecasting, 25(6), 1691-1714, doi: 10.1175/2010WAF2222417.1.

Yu, R., T. Zhou, A. Xiong, Y. Zhu, and J. Li (2007), Diurnal variation of summer precipitation over contiguous China, Geophys. Res. Lett., 34, L01704, doi: 10.1029/2006GL028129.

Yu, R., Y. Xu, T. Zhou, and J. Li (2007), Relation between rainfall duration and diurnal variation in the warm season precipitation over central eastern China, Geophys Res Lett, 34, L13703, doi: 10.1029/2007GL030315.

Zheng, Y., J. Chen, M. Chen, Y. Wang, and Q. Ding (2007), Statistic characteristics and weather significance of infrared TBB during May-August in Beijing and its vicinity, Chinese Science Bulletin, 52(24), 3428-3435, doi: 10.1007/s11434-007-0438-z.

Acknowledgments

This work was supported by the National Natural Science Foundation of China under grant 41075036.